Pathologic mechanisms of type 1 VWD mutations R1205H and Y1584C through in vitro and in vivo mouse models

Cynthia M. Pruss,[1] Mia Golder,[1] Andrea Bryant,[1] Carol A. Hegadorn,[1] Erin Burnett,[1] Kimberly Laverty,[1] Kate Sponagle,[1] Aly Dhala,[1] Colleen Notley,[1] Sandra Haberichter,[2,3] and David Lillicrap[1]

[1]Department of Pathology and Molecular Medicine, Queen's University, Kingston, ON; [2]BloodCenter of Wisconsin, Milwaukee, WI; and [3]Department of Pediatrics, Medical College of Wisconsin, Milwaukee, WI

Type 1 VWD is the mild to moderate reduction of VWF levels. This study examined the mechanisms underlying 2 common type 1 VWD mutations, the severe R1205H and more moderate Y1584C. In vitro biosynthesis was reduced for both mutations in human and mouse VWF, with the effect being more severe in R1205H. VWF knockout mice received hydrodynamic injections of mouse *Vwf* cDNA. Lower VWF antigen levels were demonstrated in both homozygous and heterozygous forms for both type 1 mutations from days 14-42. Recombinant protein infusions and hydrodynamic-expressed VWF propeptide to antigen ratios demonstrate that R1205H mouse VWF has an increased clearance rate, while Y1584C is normal. Recombinant ADAMTS13 digestions of Y1584C demonstrated enhanced cleavage of both human and mouse VWF115 substrates. Hydrodynamic-expressed VWF shows a loss of high molecular weight multimers for Y1584C compared with wild-type and R1205H. At normal physiologic levels of VWF, Y1584C showed reduced thrombus formation in a ferric chloride injury model while R1205H demonstrated similar thrombogenic activity to wild-type VWF. This study has elucidated several novel mechanisms for these mutations and highlights that the type 1 VWD phenotype can be recapitulated in the VWF knockout hydrodynamic injection model. (*Blood*. 2011;117(16):4358-4366)

Introduction

The large multimeric glycoprotein VWF is critical to normal hemostasis through mediating platelet-subendothelial interactions as well as binding to platelets to support their aggregation at the site of endothelial damage. The disease phenotype of type 1 VWD is a mild to moderate quantitative reduction of supposedly functionally normal VWF, with plasma VWF levels between 5% and 50% of normal.[1] This disease can be caused by a wide array of defects including defective RNA or protein synthesis, premature protein degradation before cellular release, ineffective secretion, rapid plasma clearance, or a mutation that results in a null allele.[2]

R1205H, the Vicenza mutation, has a relatively severe type 1 phenotype that involves accelerated VWF clearance. Often occurring with a second VWF variation, M740I, the Vicenza mutation shows a significant reduction in VWF antigen (VWF:Ag) to ~ 0.15 U/mL, VWF Ristocetin Cofactor Activity (VWF:RCo) ~ 0.20 U/mL, and Factor VIII levels < 0.30 U/mL, but maintains normal platelet VWF levels and function.[3-6] Patient bleeding scores, a marker of VWD severity, range between 2-17 (n = 18), with a mean of 8 (bleeding score ≥ 4 is positive).[1,7-9] Accelerated clearance of the mutant protein has been demonstrated via desmopressin (DDAVP) studies[3] and human recombinant protein infusion in the VWF knockout mouse,[10] as well as through high VWFpp/VWF:Ag ratios, with observed ratios of 10 or greater for this indirect measurement of VWF clearance from the plasma.[4] R1205H VWF also often displays an increase in high molecular weight multimers along with occasional alteration in the typical multimer triplet band pattern,[3-5,11] and has been attributed to the rapid clearance of the protein and thus reduced opportunity for proteolytic remodeling.[12] Patients with the R1205H mutation also have a normal or enhanced DDAVP response because there is normal Weibel-Palade body storage and release.[13,14]

The commonly occurring Y1584C mutation has a mild type 1 VWD phenotype. This mutation was first identified in 14% of index cases during the Canadian type 1 VWD study with an associated founder polymorphic haplotype.[15,16] Heterozygous patients have a mean VWF:Ag of 0.40 U/mL, and possess predominately group O blood type.[15] The Y1584C mutation was also found in 8% of index cases in the European Molecular and Clinical Markers for Diagnosis and Management (MCMDM)–1VWD study, with VWF:Ag levels ranging from 0.21-0.80 U/mL.[8] Patient bleeding scores range between 0-20 (n = 23) with a mean of 4, showing a highly variable but generally mild phenotype.[1,8,9] In vitro studies show that Y/C1584 and C/C1584 patient plasma has enhanced ADAMTS13-mediated proteolysis, although this susceptibility is much lower than that of type 2A group II VWD mutations.[17,18] In addition, in vitro expression studies in COS-7 cells have shown a reduction in VWF synthesis and increase in intracellular retention.[15]

The VWF knockout mouse has been used recently to examine several different human VWD mutations through the establishment of mouse VWF expression by hydrodynamic delivery of the mouse *Vwf* cDNA. The homogeneous, inbred genotype of the mice, relatively low cost to introduce new mutations, and the ability to evaluate larger study populations than would be available for human subjects makes this a valuable and convenient methodology to examine different VWD mutations. This approach also allows

Submitted August 25, 2010; accepted January 26, 2011. Prepublished online as *Blood* First Edition paper, February 23, 2011; DOI 10.1182/blood-2010-08-303727.

The publication costs of this article were defrayed in part by page charge payment. Therefore, and solely to indicate this fact, this article is hereby marked "advertisement" in accordance with 18 USC section 1734.

sequence changes to be examined on the background of a consistent (nonpolymorphic) cDNA sequence. This experimental strategy has already recapitulated the human disease phenotypes for defective binding to collagen and GPIIbIIIa,[19] and type 2B VWD.[20,21] However, until now, quantitative VWD phenotypes have not been explored using this methodology.

Both R1205H and Y1584C have been well described in type 1 VWD patient populations. However, neither mutation has been examined for longer-term expression in an animal model system to evaluate the associated pathogenic mechanisms in a controlled setting. This study examines through both in vitro and in vivo strategies the impact of the severe R1205H and mild Y1584C type 1 VWD mutations in mouse models of the phenotype.

Methods

Plasmid construction and mutagenesis

Full-length human VWF was produced using pCIneoVWF-ESN.[22] The mouse *Vwf* cDNA (courtesy of Peter Lenting, Inserm U770 and Université Paris-Sud, Le Kremlin-Bicêtre, France) was cloned into the pCIneo plasmid for recombinant protein and into the pSC11 plasmid[23] with the liver-specific Enhanced murine Transthyretin (ET) promoter (courtesy of Luigi Naldini, San Raffaele Telethon Institute for Gene Therapy, San Raffaele Scientific Institute, Milan, Italy)[24] for hydrodynamic delivery. hVWF115, a GST and histidine tagged 115 amino acid fragment of the VWF A2 domain, E1554-R1668, was constructed from the pGEX-6P-1 backbone (GE Healthcare Life Sciences) and pCIneoVWF-ESN, with mVWF115 being produced in a similar manner.[25] Site-directed mutagenesis was performed using the Quikchange XL II kit (Stratagene). Both R1205 and Y1584 are conserved between human and mouse. Mouse *Adamts13* cDNA (courtesy of Dr F. Scheiflinger, Baxter, Austria) was cloned into the pSC11 plasmid[23] with the liver-specific ET promoter[24] for hydrodynamic delivery.

Recombinant protein production and cell culture

HEK293T and COS-7 cells were transiently transfected using the calcium phosphate method and ATt-20 cells were transfected using Lipofectamine (Invitrogen) as previously described.[15,22] A total of 10 μg of *VWF* cDNA plasmid was transfected per 10-cm dish, consisting of wild-type, R1205H, Y1584C, or cotransfections of 5 μg of wild-type and mutant cDNA. VWF was secreted into serum-free OptiMEM containing 100 U/mL penicillin, 100 μg/mL streptomycin, 1X Insulin/Selenium/Transferrin G (Invitrogen). Medium was harvested after 72 hours and recombinant VWF was concentrated using Amicon Ultra-15 or Ultra-70 100K MWCO units (Millipore). Medium and cellular lysates from individual 10 cm dishes were evaluated for VWF protein levels.

Human and mouse ADAMTS13 derived from the pcDNA3.1-hADAMTS13 and pcDNA3.1-mADAMTS13 expression vectors (gifts of Dr F. Scheiflinger) were produced via stable transfection in HEK293T cells similar to the recombinant VWF, using G418 selection.[26] ADAMTS13 activity was determined using the ADAMTS13 activity ELISA Kit (Japan Clinical Laboratories).[27] The VWF115 proteins were produced in BL21-Gold *Escherichia coli* (Stratagene) and purified via Ni-NTA agarose (QIAGEN).[22]

VWF antigen, propeptide, and multimer quantitation

VWF protein concentration was determined by VWF ELISA using polyclonal human VWF antibodies A0082 and P0226 (DAKO). Human VWF concentration was assayed against a standard human plasma pool (CRYOcheck; Precision Biologic). Mouse VWF propeptide (VWFpp) concentration was determined using the 349.3 capture antibody, and detected via the horseradish peroxidase-linked 349.2 antibody, both provided by S.H. Mouse VWF, VWF propeptide, and ADAMTS13 activity concentrations were determined using a normal C57Bl/6 mouse plasma pool, derived from 25 normal, 8-week-old, mixed gender, C57Bl/6 mice, with the means arbitrarily determined to be 1 U/mL mVWF, mVWFpp, and mADAMTS13.

VWF multimers were analyzed by electrophoresis using a 1.4% separating SDS agarose gel and visualized using the VWF antibody P0226 (DAKO) as previously described.[28] Lanes were analyzed by 1-D densitometry for multimer distance and band number using AlphaEaseFC Version 3.1.2 (Alpha Innotech).[22] Multimer films were scanned using HP Scanjet G4010 (Hewlett-Packard) and figures created using Adobe Illustrator CS4 Version 14.0.0 (Adobe Systems Inc).

In vitro ADAMTS13 digests of recombinant VWF

For full-length hVWF digestion, recombinant human ADAMTS13 (hADAMTS13) was diluted 2-fold in 5mM Tris (tris(hydroxymethyl)aminomethane), pH 8.0, and activated with 10mM $BaCl_2$ final concentration for 5 minutes at 37°C. A 100-μL aliquot of hADAMTS13 was added to 100 μL rVWF, 1 U/mL in 5mM Tris, pH 8.0, and dialyzed against 1.5M urea, 5mM Tris, pH 8.0, on VSWP02500 filters (Millipore). After 5 hours, the samples were collected and 25mM EDTA (ethylenediaminetetraacetic acid), final concentration, was added.

For full-length mVWF digestion, recombinant mouse ADAMTS13 (mADAMTS13) was diluted 2-fold in 5mM Tris, pH 8.0 and activated with 10mM $BaCl_2$ for 5 minutes at 37°C. 25 μL of mADAMTS13 was added to 25 μL of rVWF (1 U/mL in 1.5M urea, 5mM Tris) and incubated for 24 hours at 37°C. EDTA at a final concentration of 50mM was added to stop the reaction.[29] Samples were frozen at −80°C until multimer analysis. Analysis of the relative multimer migration for full-length digests was analyzed as previously described, using a 4-parameter curve fit to determine EC_{50}, or ADAMTS13 concentration to cause 50% loss of relative multimer distance.[29] Curve fit F tests for $\log EC_{50}$ were performed to determine statistical significance.

The hVWF115 and mVWF115 ADAMTS13 digestion ELISA assays were modified from the ADAMTS13 activity ELISA.[27] Reacti-Bind Anti-GST plates (Pierce) were coated with 1.25 mg/mL VWF115 in PBS, pH 7.2 for 1 hour, and washed with PBS/0.05% Tween-20 (PBS/Tween). 2-fold dilutions of ADAMTS13 were made in 5mM acetate, 5mM $MgCl_2$, pH 5.5 and added to each well for 4 hours at 37°C, the wells were washed with PBS/Tween, and 1 μg/mL HISProbe (Pierce) in PBS/Tween was added for 1 hour. 1X OPD reagent (Sigma-Aldrich) was used for visualization, the reaction stopped at 10 minutes with 2.5M H_2SO_4, and absorbance was read at 492 nm. EC_{50}, the ADAMTS13 concentration to digest half the VWF115 substrate, was determined via 4-parameter curve fit. A *t* test of the mean EC_{50} values was performed to determine statistical significance.

VWF studies in VWF knockout mice

VWF knockout mice[30] on a C57Bl/6 background (The Jackson Laboratory) aged 8 to 10 weeks, were used in all experiments. All mouse experiments were reviewed and approved by the Queen's University Animal Care Committee.

Hydrodynamic injections

Plasmid DNA was diluted in a 10% body weight volume of lactated Ringer solution and injected via tail vein in less than 7 seconds using a 27-gauge needle and a 3-mL syringe. VWF knockout mice were 8-9 weeks of age at the time of injection. Wild-type, R1205H, and Y1584C mice received 100 μg of *Vwf* cDNA plasmid, pSC11-ET-mVWF. Wild-type/R1205H and wild-type/Y1584C mice received 50 μg of wild-type and 50 μg mutant plasmid in coinjection studies. VWF and ADAMTS13 coinjections received 50 μg of *Vwf* cDNA and 20 μg *Adamts13* of cDNA.

Blood collection

Blood was collected using a 70-μL untreated glass capillary tube via retrorbital plexus under isofluorane/oxygen anesthetic using 10% buffered

citrate as anticoagulant. Blood was centrifuged at 11 000g for 5 minutes to generate platelet poor plasma, and samples stored at −80°C until tested.

Recombinant mVWF protein infusions

Recombinant mouse VWF was infused into mice at 0.2 U/g weight via tail vein in saline. Each mouse was sampled once, with a minimum of 3 animals per time point. Data were fit to a 1-phase exponential decay with plateau phase and curve fit F test for half-life used to determine statistical significance.

Intravital microscopy for the ferric chloride injury model of thrombosis

Intravital microscopy was performed using a trinocular Wild-Leitz ELR-intravital microscope (Leica Microsystems Canada), fitted with transmitted (50W halogen) and fluorescence (50W mercury incidence) light accessories. Images of thrombus formation were captured by a Hamamatsu ORCA ER video camera (Bridgewater) with fluorescent light. Analysis of the formed thrombi and the accumulated fluorescence intensity was performed using Image Pro Plus Version 6.0 (Media Cybernetics).

Ferric chloride injury was induced as described previously.[21,31,32] Male mice were anesthetized via intraperitoneal injection of ketamine/xylazine/atropine. The jugular vein was cannulated for injection of rhodamine 6G (40 ng; Sigma-Aldrich) to fluorescently label platelets in vivo and the cremaster exteriorized. Arterioles ranging in size from 7.5 to 18 μm were chosen and after rhodamine 6G infusion, injury was induced through the application of 10% ferric chloride-soaked filter paper (1 × 1 mm) for 3 minutes. After injury, the injured area in a single arteriole was observed for 40 minutes. The time to vessel occlusion with thrombus and accumulated fluorescence intensity from images captured at 5 minute intervals were examined. Occlusion times exceeding 40 minutes were recorded as 40 minutes.

Graphing and statistical analysis

All data and statistical analysis was performed using GraphPad Prism 4.03 for Windows. Data are presented as mean values ± SEM. Statistical analyses were performed using the Student unpaired *t* test, 1-way ANOVA with the Tukey posttests or 2-way ANOVA with Bonferroni posttests, as appropriate. *P* values $< .05$ were considered statistically significant.

Results

Expression and characterization of recombinant proteins

Recombinant human VWF was produced via transient transfection in HEK293T cells (Figure 1A), as well as COS-7 and ATt-20 cells (Figure 1C-E). All values were normalized to total wild-type VWF antigen equal to 100%. Human VWF produced in HEK293T cells via transient transfection showed a decrease in total protein production for both Y1584C (69.6% of wild-type, $P < .001$) and R1205H (64.0% of wild-type, $P < .001$), although cell lysate levels were similar ($P > .05$). These reductions are less severe in cotransfections of wild-type cDNA with each mutation (modeling the heterozygous state for each mutation). Compared with wild-type VWF protein expression, wild-type/Y1584C had levels of 79.8% ($P < .05$), and wild-type/R1205H had levels of 69.8% ($P < .001$). Similar results were observed in the other 2 cell lines, with no significant differences between VWF levels in the cell lysates, but reduced levels of the secreted proteins.

Mouse VWF exhibited similar trends to human VWF (Figure 1B,D,F). In HEK293T transfections, wild-type mVWF (100.0%) was not different from that of Y1584C (104%, $P > .05$). In contrast, mouse VWF proteins, R1205H (71.2%, $P < .01$), wild-type/Y1584C (77.9%, $P < .05$), and wild-type/R1205H (83.5%, $P < .05$) all demonstrated significantly lower secretion rates than wild-type mVWF, with R1205H being the most severely reduced. Cell lysates produced similar amounts of protein ($P > .05$).

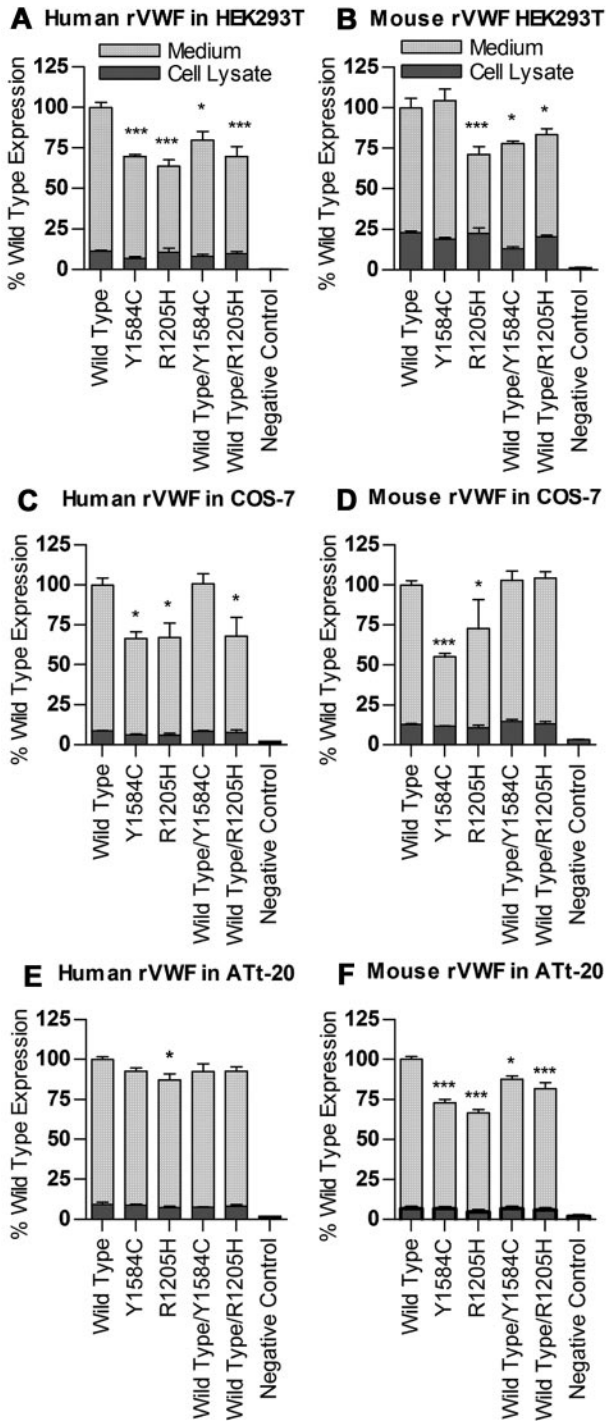

Figure 1. Expression of human and mouse recombinant VWF. Transient transfections of VWF cDNAs were performed in HEK293T, COS-7 and ATt-20 cells, and expressed in serum-free medium, 2 experiments, n = 3 each. Total VWF produced in medium and cell lysates per 10 cm dish was measured via VWF:Ag ELISA, and results normalized to total wild-type VWF equal to 100 for both human (A,C,E) and mouse (B,D,F). *$P < .05$. ***$P < .001$.

In vitro ADAMTS13 digests of recombinant VWF

Full-length VWF digests were performed in duplicate in the presence of 1.5M urea using a 2-fold dilution series of ADAMTS13 (Figure 2A-B).

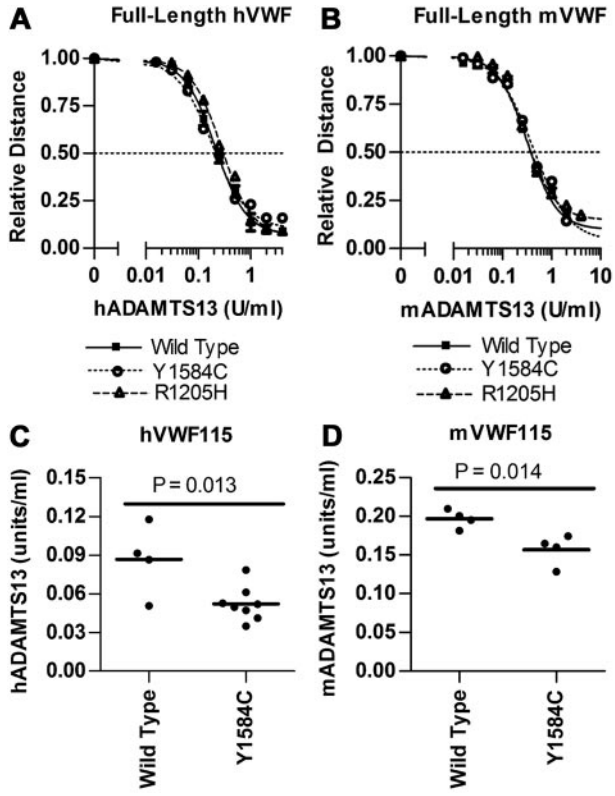

Figure 2. Analysis of ADAMTS13 digestion of full-length VWF and VWF115. Recombinant ADAMTS13 digests were performed as outlined under "In vitro ADAMTS13 digests of recombinant VWF." (A-B) Varying concentrations of ADAMTS13 were incubated with 1 U/mL full-length VWF for 24 hours with 1.5M Urea. Multimer graphs for wild-type, Y1584C, and R1205H VWF were plotted using a 4-parameter curve fit. The concentration of ADAMTS13 required to cause a 50% loss of multimer height was determined. Symbols represent mean values and SE from 2 experiments. (C-D) Comparison of the ADAMTS13 concentrations necessary for 50% loss of intact human and mouse VWF115. Varying ADAMTS13 concentrations were incubated with VWF115 for 4 hours under nondenaturing conditions. Bars represent the mean values, and each circle represents a separate assay.

Human full-length VWF digests showed no significant difference between wild-type (1.71 U/mL hADAMTS13), Y1584C (1.67 U/mL, $P = .85$), or R1205H (2.10 U/mL hADAMTS13, $P = .12$). Mouse full-length VWF digests also resulted in no significant difference in EC50 values between wild-type (0.341 U/mL mADAMTS13), R1205H (0.371 U/mL mADAMTS13, $P = .34$) and Y1584C (0.423 U/mL mADAMTS13, $P = .30$).

VWF115 digests of wild-type and Y1584C protein were performed under nondenaturing conditions (Figure 2C-D). R1205H was excluded from these studies, because this change is outside the region in VWF115. The hADAMTS13 had cleaved 50% of wild-type hVWF115 at 0.0865 U/mL hADAMTS13, and Y1584C required 40% lower hADAMTS13 levels at 0.0521 U/mL ($P = .013$). Mouse ADAMTS13 had cleaved 50% of wild-type mVWF115 at 0.197 U/mL mADAMTS13, while Y1584C required 21% lower mADAMTS13 levels at 0.157 U/mL ($P = .014$).

Recombinant mouse VWF protein infusions

Mice were infused with recombinant mouse VWF (0.2 U/gm body weight), and a minimum of 3 mice were sampled per time point. Data were fit to a 1-phase exponential decay with plateau phase, the best fitting model for the data (Figure 3). The half-life for wild-type protein was 35.1 minute, Y1584C was 40.8 minutes ($P = .64$) and for R1205H was significantly reduced at 21.9 minutes ($P < .0001$).

Hydrodynamic injections

VWF knockout mice received plasmid DNA containing the liver-specific ET promoter and mouse *Vwf* cDNA. This results in hepatocyte-specific expression of the mouse VWF protein, which presumably has an altered glycan content compared with normal endothelial and platelet-derived VWF. This transgene delivery method replaces only the plasma component of VWF content in the knockout animals. Complete blood counts (CBCs) were performed with all *Vwf* cDNA combinations tested. A transient thrombocytopenia was observed on day 2 after transgene administration, with full recovery after all injections by day 5. No other adverse events or alterations in CBC values were observed (data not shown).

VWF antigen levels

VWF:Ag levels reached maximum levels 2 days after hydrodynamic injection (Figure 4A). Wild-type VWF:Ag reached a level of 25.0 U/mL, while R1205H was 35% lower at 16.3 U/mL ($P < .001$). Both Y1584C and wild-type/R1205H heterozygotes were not significantly different from wild-type VWF:Ag levels (27.2 U/mL and 25.7 U/mL, respectively, $P > .05$). The level in wild-type/Y1584C heterozygotes was significantly higher at 39.9 U/mL ($P < .001$). The initial peak VWF:Ag levels declined to a more stable slow decay phase by day 14, at which point mice that had received the wild-type VWF cDNA had the highest VWF:Ag expression levels through days 14 to 42 (Figure 4B-C). From day 14 onward, the 2 type 1 VWD mutations, either alone or coexpressed with wild-type VWF (representative of the heterozygous state), demonstrated lower VWF:Ag levels. R1205H VWF:Ag levels were an average 34% of wild-type VWF ($P < .001$) from days 14 to 42, and wild-type/R1205H were 27% ($P < .001$). Y1584C VWF:Ag levels were 29% of wild-type ($P < .001$), while wild-type/Y1584C levels were 51% ($P < .001$). Results from days 21 and 28 (Figure 4C) show the variability between the individual animals in the study, compared with the mean values.

VWF propeptide to VWF antigen ratios

VWF propeptide levels were measured, and followed a similar expression profile to that of VWF:Ag, with maximum levels on day

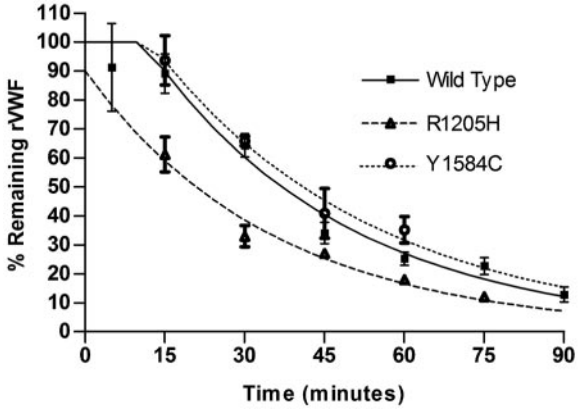

Figure 3. Recombinant mouse protein clearance. Recombinant mouse VWF protein (0.20 U/g) was injected via tail vein into VWF knockout mice. Mice were sampled once ($N \geq 3$ mice per time point). Data are reported as % remaining recombinant mouse VWF. Half-life was determined for each recombinant VWF protein.

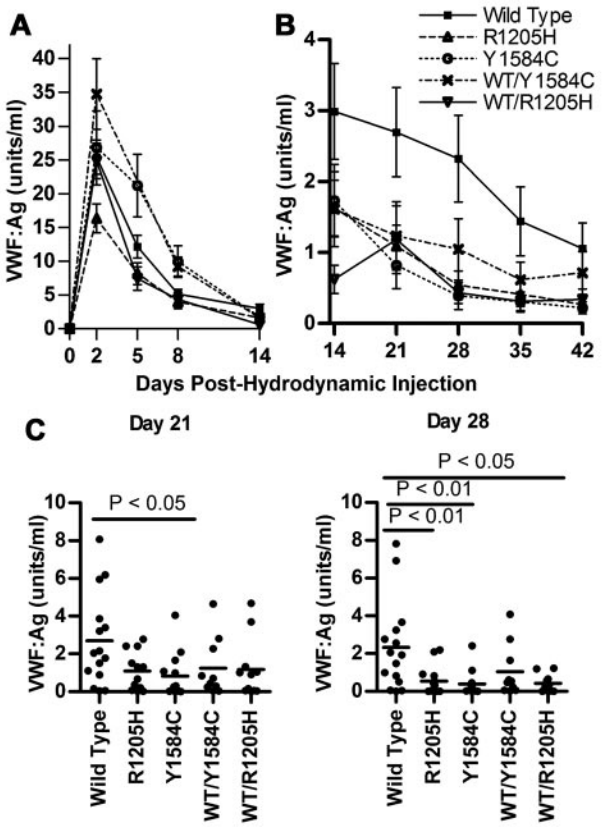

Figure 4. Mouse VWF antigen levels after hydrodynamic injection. VWF knockout mice expressing wild-type, R1205H, Y1584C, or wild-type and mutant mVWF were sampled after thydrodynamic injection (N ≥ 10). VWF:Ag levels were determined via ELISA. (A) VWF:Ag levels from days 2 to 14 after hydrodynamic injection. (B) VWF:Ag levels from days 14 to 42 after hydrodynamic injection. Symbols represent means with SEM error bars. (C) VWF:Ag levels for days 21 and 28. Each circle represents data from a single mouse; bars represent the mean VWF:Ag value.

2, and a slow decay phase from day 14 onward (data not shown). VWFpp/VWF:Ag ratio was determined, with a mean value of 1 being equal to the mean of wild-type VWFpp/VWF:Ag ratios from days 2 to 42 (Figure 5). This value was 6.5-fold lower than that of the observed mean VWFpp/VWF:Ag ratio obtained from plasma of normal C57Bl/6 mice. The VWFpp/VWF:Ag ratio for Y1584C was not significantly different from that of wild-type VWF, with mean ratio values of 0.97 versus 1.00 ($P > .05$). R1205H, however, did demonstrate an increased mean VWFpp/VWF:Ag ratio of 1.65 ($P < .001$). The coexpression of wild-type and mutant *VWF* cDNAs had VWFpp/VWF:Ag ratios similar to wild-type ($P > .05$, data not shown). Coexpression of *Adamts13* cDNA with wild-type or mutant *VWF* cDNA produced VWFpp/VWF:Ag ratios were not significantly different from wild-type *VWF* cDNA alone, ($P > .05$, data not shown).

Multimeric structure

Multimeric profiles of the liver-expressed mVWF were examined to determine whether the mutations altered the VWF multimer structure. The mouse VWF produced from the liver, after hydrodynamic injection, has an altered multimer appearance compared with that of normal mouse plasma (Figure 6A). Single multimer bands rather than a normal triplet structure were observed, with a slightly lower molecular weight for each band, and occasional faint lower bands. In addition, the multimer profile was skewed toward lower molecular weight multimers compared with normal mouse plasma.

Multimer band number counts were used to quantify differences in multimeric structure (Figure 6B). Wild-type VWF had a peak level of 22 bands at day 2, and a low of 8.57 bands at day 28, with an average band number of 12.54. R1205H had an average of 11.69 bands, a decrease of 0.85 bands compared with wild-type ($P > .05$). In contrast, Y1584C had an average of 8.31 multimer bands, a significant decrease of 4.23 bands ($P < .001$).

Animals receiving coinjected *Vwf* and *Adamts13* cDNAs via hydrodynamic delivery (to compensate for the truncated and functionally defective ADAMTS13 in C57Bl/6 mice) had a diminished multimer size (Figure 6C). ADAMTS13 activity in these mice was determined using m73 substrate with an antibody that detects intact A2 domain substrate, in a static activity assay. Mouse ADAMTS13 levels were found to be an average of 5.92 U/mL on day 5, 4.14 U/mL on day 8 and 5.14 U/mL on day 14 (data not shown). With the coinjected *Adamts13* cDNA, wild-type VWF had an average band number of 9.38 from days 5-14. R1205H had a slightly higher molecular weight multimer structure with 10.2 bands ($P > .05$). In contrast, Y1584C showed a significant decrease to 5.08 bands ($P < .01$), demonstrating that the addition of full-length ADAMTS13 to the VWF knockout mouse exaggerates the abnormal multimer structure for Y1584C.

Evaluation of in vivo thrombogenesis

Performance of the ferric chloride injury model of thrombosis on cremaster arterioles demonstrated a marked difference in mean occlusion times for both type 1 VWD mutations studied, although their plasma levels at the time of evaluation were similar to wild-type VWF (Figure 7). All mice were expressing VWF:Ag levels between 0.5 and 2.4 U/mL mVWF at the time of thrombogenesis testing. The Y1584C VWF mice had a much longer time to occlusion compared with wild-type (38.7 vs 29.9 minutes, $P = .001$, Figure 7A). In contrast,

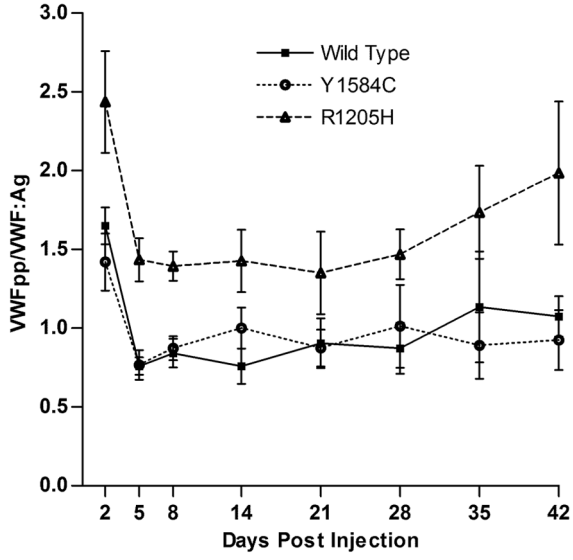

Figure 5. VWFpp/VWF:Ag ratios for hydrodynamic mVWF VWF knockout mice expressing wild-type, R1205H, or Y1584C cDNA were sampled after hydrodynamic injection (N ≥ 10). VWF:Ag and VWFpp levels were determined via ELISA. Values are normalized to a mean wild-type ratio equal to 1.0, which is 6.5-fold lower than that of normal C57BL/6J mice.

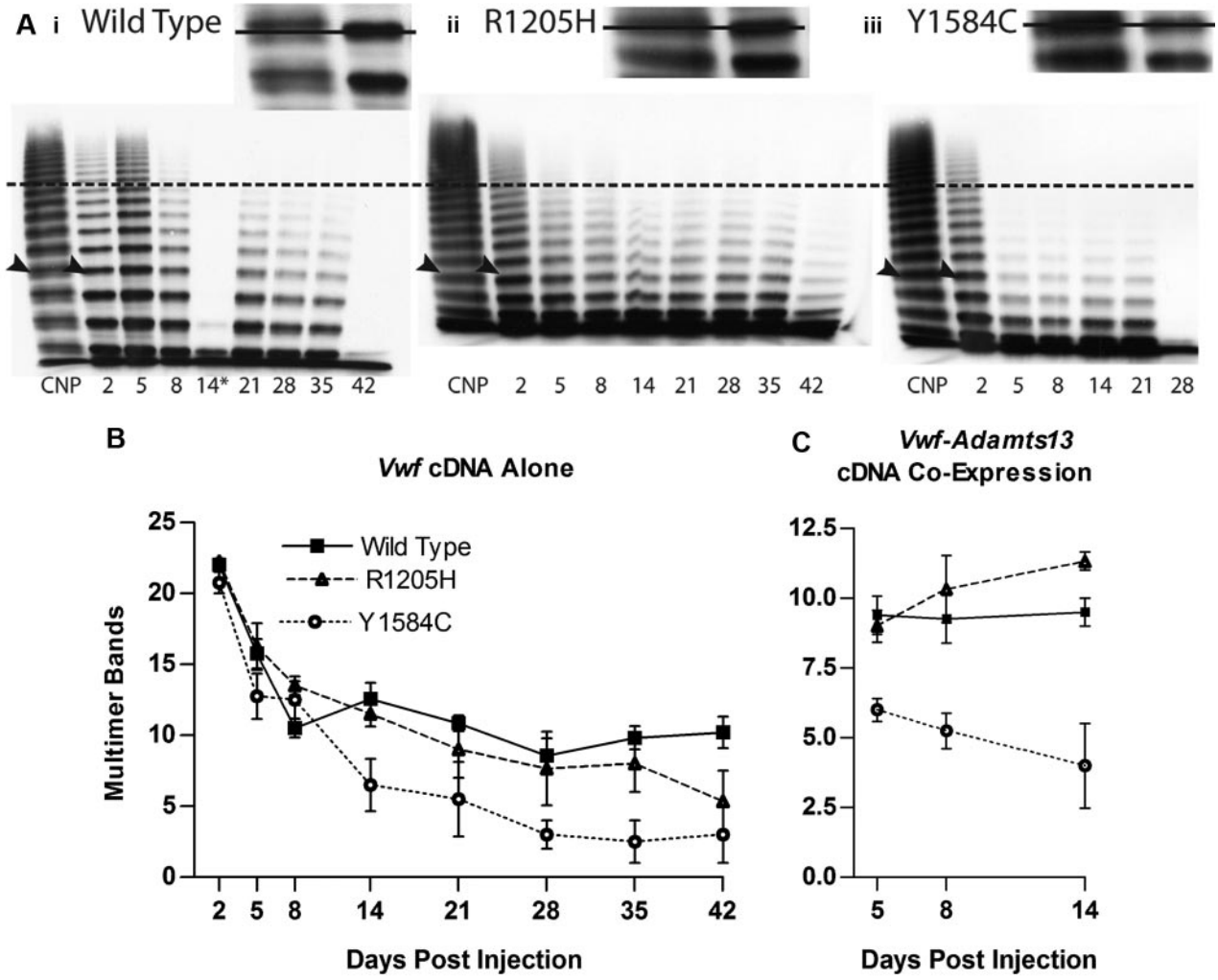

Figure 6. Hydrodynamic mVWF multimer structure. VWF knockout mice expressing wild-type, R1205H, or Y1584C mouse VWF were sampled after hydrodynamic injection and evaluated for multimeric structure. Plasma was run on a 1.4% agarose gel at an mVWF concentration of 1.0 U/mL. (A) Exemplar multimers are shown for (i) wild-type, (ii) R1205H, and (iii) Y1584C. The dotted line represents high molecular weight multimers, greater than 10 multimer bands. Arrowheads indicate the top bands in the enlarged inset bands, with a line through the inset figure illustrating the single band of lower molecular weight in the recombinant proteins compared with C57Bl/6 normal plasma pool (CNP) triplet multimer bands. The asterisk (*) denotes a multimer from a clotted sample. Wild-type day 42 and Y1584C day 28 samples were less than 1 U/mL. (B) Multimer analysis was performed on VWF knockout mice expressing mVWF after hydrodynamic injection by counting the total number of resolved multimer bands in each lane. N ≥ 4. (C) Multimer analysis on VWF knockout mice expressing mVWF and mADAMTS13 after hydrodynamic injection. N ≥ 4.

studies with the R1205H mutant showed variable occlusion times but a mean value similar to that observed in wild-type mice (29.1 minutes, $P > .05$). Total relative platelet accumulation was also lower for Y1584C compared with wild-type (38.5 vs 47.1, $P = .043$), while R1205H was similar to wild-type (48.8, $P = .72$, Figure 7C)

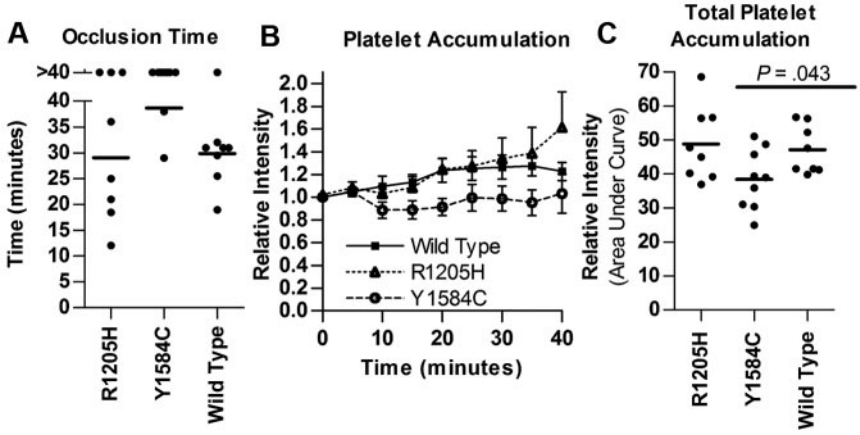

Figure 7. Thrombogenesis in response to ferric chloride injury. VWF knockout mice expressing VWF cDNA after hydrodynamic injection with VWF:Ag levels between 0.5 and 2.5 U/mL were evaluated using 10% ferric chloride injury to the cremaster. (A) Time to a stable occlusive thrombus. The experiment was stopped at 40 minutes, mice that failed to occlude were recorded as 40 minutes. (B) Platelet accumulation via mean relative fluorescence intensity. Mean with SEM was graphed for each dataset. (C) Total platelet accumulation. Area under the curve was determined. Each circle represents a single mouse; bars indicate mean.

Discussion

We selected 2 recurrent and contrasting type 1 VWD mutations for this study to carry out a comprehensive pathogenic characterization of the mechanisms responsible for their phenotypes. R1205H, a highly penetrant dominant mutation with a severe type 1 phenotype, was selected because it has previously been demonstrated to show an enhanced clearance mechanism. In contrast, the frequent and incompletely penetrant Y1584C mutation has a mild phenotype, and an unresolved pathogenetic mechanism. Both R1205 and Y1584 are conserved between human and mouse VWF proteins, allowing the R1205H and Y1584C mutations to be examined in the mouse model. This study has now completed a comprehensive pathogenetic evaluation to determine the relative contributions of defective biosynthesis and release, ADAMTS13-mediated proteolysis, and clearance mediated by these 2 type 1 VWD mutations. We have also evaluated the influence of the 2 mutant proteins in an in vivo thrombosis model to determine whether their functional contributions to this process are similar when plasma VWF levels are equivalent.

The defining characteristic of type 1 VWD is a proportionate decrease in both VWF:Ag and VWF:RCo levels, between 0.05 and 0.5 U/mL. It is implied from this proportionate reduction in both measurements that the low level of VWF has a normal hemostatic function. Before initiating these studies, quantitative type 1 VWD VWF mutations had not been evaluated in the mouse, so it was unclear if these changes would result in lower VWF plasma levels in this system. However, these studies have shown that in the long term slow decay phase of VWF expression from day 14 onward, VWF:Ag levels are indeed significantly decreased in both Y1584C and R1205H, thus recapitulating the difference in human phenotypes. Importantly, these low VWF:Ag levels are also observed in mice that were coinjected with mutant and wild-type cDNAs, modeling the heterozygous state observed in type 1 VWD patients.

Defective biosynthesis and secretion has been described for many VWD mutations. The Y1584C mutant had been previously demonstrated to show decreased protein synthesis and increased cellular retention in vitro using COS 7 cells.[15] In contrast, the R1205H mutation has been reported not to alter synthesis.[12] Our in vitro experiments demonstrate that both Y1584C and R1205H do adversely affect total synthesis of VWF in both the homozygous and heterozygous states to varying degrees in 3 cell lines. The quantitative biosynthetic defects are replicated with both the human and the mouse VWF constructs, but neither type 1 mutation appears to influence the generation of normal multimer structure. We also suspect that a biosynthetic defect is likely contributing to the decreased VWF:Ag levels observed in the mice expressing VWF after hydrodynamic injection. These mice show normal VWFpp/VWF:Ag ratios for the Y1584C mutant, and only 1.65-fold higher ratios in the mice expressing R1205H, suggesting that accelerated clearance of the proteins is not the only pathogenic influence in this system, unlike the situation in patients.

The effects of ADAMTS13-mediated digestion were examined by in vitro digestion of full-length and VWF115 substrates as well as by examining the multimer profiles of hydrodynamic-injection mice. The mouse VWF protein amino acid sequence has 83% identity and 91% homology to that of human VWF, with similar variation in the ADAMTS13 sequences.[29,33] Mouse ADAMTS13 has poor activity on the human VWF substrate in both full-length and A2 domain VWF73 assays.[34] This is further exacerbated by a retrotransposon insertion in C57Bl/6 mice that leads to the premature truncation of ADAMTS13.[35] Although similar activity is observed in static assays, this truncated ADAMTS13 demonstrates increased thrombotic occlusions under shear stress conditions, because it is not fully active in vivo.[36] To mitigate any artifacts caused by these differences, we digested both human and mouse substrates with their respective species-specific ADAMTS13. In addition, we performed coinjections of full-length mouse *Adamts13* cDNA with the *Vwf* cDNAs to observe any influences on the VWF multimer profile or clearance rate in vivo. However, this coexpression method will not elucidate if a decrease in high molecular weight VWF is because of an interaction intracellularly or in the circulation with the additional hepatocyte expression of ADAMTS13.

The R1205H mutant protein showed no alteration in the full-length VWF ADAMTS13 digestions and multimer profiles in the hydrodynamically injected mice were also normal for R1205H. Thus, the R1205H mutation does not influence the cleavage of VWF by ADAMTS13.

In contrast, Y1584C displays a mild type 2A group II VWD phenotype in our study. Although the full-length digests did not show a difference in cleavage rates, the in vitro VWF115 assays did show an enhanced cleavage profile for Y1584C, and Y1584C expressing mice had reduced multimer band numbers that was exacerbated by coinjection of the m*Adamts13* cDNA. These results support patient plasma studies that have shown that the Y1584C protein is more susceptible to ADAMTS13-mediated proteolysis.[17,18] This enhanced cleavage could explain the disproportionately higher bleeding scores reported in some Y1584C individuals, who usually have only mildly reduced VWF:Ag levels.[1]

Increased protein clearance is now recognized as a pathogenic mechanism that contributes to the type 1 VWD phenotype. R1205H has consistently been shown to have a greatly shortened half-life in patients. This finding has been complemented through the premature clearance of radio-labeled R1205H human VWF protein in the VWF knockout mouse.[10] Our study examined recombinant mVWF protein clearance rates as well as VWFpp/VWF:Ag ratios in the hydrodynamically injected mice, an indirect measure of VWF clearance. The relatively short half-lives of the recombinant protein infusions do not represent the circulation time for normal mouse plasma VWF (most likely because of glycosylation differences in HEK293T cell-derived VWF), but the evaluation of the 3 recombinant molecules using the same experimental protocol provides a valid approach to comparing their half-lives. The infused recombinant R1205H had a significantly shorter half-life compared with wild-type recombinant protein, with a 27% decrease. This is not as dramatic as that observed using radiolabeled human R1205H VWF, which had a 90% decrease in mean residence time compared with wild-type human VWF.[10] This more discrepant result could be because of inherent species differences in the VWF molecules. Infused Y1584C protein did not show a significant change in half-life from wild-type VWF and VWFpp/VWF:Ag ratios for Y1584C were also similar to the results of wild-type VWF in the hydrodynamic-injection mice. R1205H showed an elevated VWFpp/VWF:Ag ratio of 1.65, but this was much lower than the ratios seen in R1205H patients, that are often greater than 10.[4] This difference appears to be due, in part, to the system used to express the plasma VWF in these mice, which also results in a 6.5-fold decrease in the VWFpp/VWF:Ag ratio for wild-type VWF compared with the ratio in normal C57Bl/6 mouse plasma. It is possible that clearance mechanisms in the mouse were already saturated, leading to a less severe increase in clearance rate with the R1205H mutant.

We have also evaluated the procoagulant function of the 2 mutant proteins in an established in vivo thrombosis model in the hydrodynamically injected mice. These studies were carried out at similar plasma levels of the proteins to eliminate the influence of VWF concentration. These results from the thrombosis injury model highlight the paradoxical severities of the plasma VWF levels and hemostatic responses associated with these 2 mutations. While R1205H has a relatively severe phenotype based on VWF:Ag and VWF:RCo levels, the protein produces similar results to wild-type VWF in the thrombogenesis studies. In contrast, Y1584C has a mild phenotype based on VWF:Ag and VWF:RCo levels but consistently showed reduction of platelet accumulation and a loss of vessel occlusion in the thrombosis injury model. This may well be because of the loss of higher molecular weight multimer structure secondary to increased ADAMTS13 cleavage of the Y1584C mutant. This influence on in vivo clot formation could explain the enrichment of this mild quantitative variant in populations of type 1 VWD. These findings also suggest that clinical symptoms may be relatively mild with the R1205H mutation, but that patients with the Y1584C variant may be overrepresented in bleeding populations in relation to their VWF levels.

In this study, the Y1584C mutant demonstrated decreased biosynthesis in vitro, enhanced proteolysis by ADAMTS13 in vitro and in vivo, and decreased VWF plasma levels in vivo. The increase in ADAMTS13-mediated cleavage produced a mild type 2A VWD multimer profile that probably contributed to the delay in forming occlusive thrombi in our ferric chloride injury model. In contrast, the R1205H mutant demonstrated decreased biosynthesis, increased protein clearance, but no alteration in ADAMTS13-mediated cleavage. Moreover, the protein when expressed at normal physiologic levels demonstrated similar occlusion times to that of wild-type VWF in the ferric chloride model, showing that at normal concentrations the R1205H VWF protein behaves normally in thrombogenesis.

Significantly, these studies demonstrate that multiple approaches are necessary to determine the complex pathogenic mechanisms underlying type 1 VWD. In the study of these 2 type 1 VWD mutants, we documented evidence of decreased VWF biosynthesis, increased ADAMTS13 cleavage, enhanced clearance, and a differential contribution to in vivo thrombogenesis.

The question remains if this is an accurate portrayal of the human disease. Although there are limitations in using this in vivo expression system, we feel that the ability to rapidly generate multiple changes at a low cost and to see the effects in an easily evaluated manner overcomes these limitations. In addition, this methodology allows a greater range of testing beyond only a few in vitro readouts, or studies on small numbers of genetically heterogeneous patients carrying a specific *VWF* mutation, currently the standard approaches for determination of the pathogenic mechanism in this condition.

These findings extend current pathophysiologic knowledge for type 1 VWD mutations and provide a practical approach to furthering our understanding of the mechanisms underlying this quantitative trait. We have established that the VWF knockout hydrodynamic delivery approach provides a practical means to evaluate defects in VWF clearance rates, decreased biosynthesis, and ADAMTS13-mediated cleavage, combined defects of which may contribute to the generation of the type 1 VWD phenotype.

Acknowledgments

The authors thank Robert Montgomery for the mouse VWFpp antibodies, Peter Lenting for the mouse *VWF* cDNA, Friedrich Scheiflinger for the mouse ADAMTS13 expression vector, Luigi Naldini for the synthetic ET promoter, and Jeff Mewburn and Jalna Meens (Queen's Cancer Research Institute) for help with the intravital microscopy studies. We thank Christine Brown for performing the VWF transfections in COS-7 and ATt-20 cell lines.

This work was supported by funds from the Canadian Institutes of Health Research (operating grant MOP-97849; D.L.) and from The National Institutes of Health (program project grant HL081588; D.L., S.H.). C.M.P. is the recipient of an Ontario Graduate Studentship and Heart and Stroke Foundation of Ontario Master's Studentship. D.L. holds a Canada Research Chair in Molecular Hemostasis.

Authorship

Contribution: C.M.P. designed, performed, analyzed, and interpreted research, performed statistical analysis, and wrote the manuscript; M.G. and A.D. performed and analyzed research; A.B., C.A.H., E.B., K.L., C.N., and K.S., performed research; S.H. provided VWF propeptide antibodies, and D.L. designed research, interpreted data, and wrote the manuscript.

Conflict-of-interest disclosure: The authors declare no competing financial interests.

Correspondence: David Lillicrap, Department of Pathology and Molecular Medicine, Richardson Laboratory, Queen's University, Kingston, ON, K7L 3N6 Canada; e-mail: lillicrap@cliff.path.queensu.ca.

References

1. Goodeve AC. The genetic basis of von Willebrand disease. *Blood Rev.* 2010;24(3):123-134.
2. Lillicrap D. Genotype/phenotype association in von Willebrand disease: Is the glass half full or empty? *J Thromb Haemost.* 2009;7 suppl 1:65-70.
3. Casonato A, Pontara E, Sartorello F, et al. Reduced von Willebrand factor survival in type Vicenza von Willebrand disease. *Blood.* 2002; 99(1):180-184.
4. Haberichter SL, Castaman G, Budde U, et al. Identification of type 1 von Willebrand disease patients with reduced von Willebrand factor survival by assay of the VWF propeptide in the european study: Molecular and clinical markers for the diagnosis and management of type 1 VWD (MCMDM-1VWD). *Blood.* 2008;111(10):4979-4985.
5. Casonato A, Pontara E, Sartorello F, et al. Identifying type Vicenza von Willebrand disease. *J Lab Clin Med.* 2006;147(2):96-102.
6. d'Alessio PA, Castaman G, Rodeghiero F, et al. In vivo experiments indicate that relatively high platelet deposition in von Willebrand's disease 'Vicenza' is caused by normal platelet-VWF levels rather than by high VWF-multimers in plasma. *Thromb Res.* 1992;65(2):221-228.
7. Bowman M, Mundell G, Grabell J, et al. Generation and validation of the condensed MCMDM-1VWD bleeding questionnaire for von Willebrand disease. *J Thromb Haemost.* 2008;6(12):2062-2066.
8. Goodeve A, Eikenboom J, Castaman G, et al. Phenotype and genotype of a cohort of families historically diagnosed with type 1 von Willebrand disease in the European study, molecular and clinical markers for the diagnosis and management of type 1 von Willebrand disease (MCMDM-1VWD). *Blood.* 2007;109(1):112-121.
9. Tosetto A, Rodeghiero F, Castaman G, et al. A quantitative analysis of bleeding symptoms in type 1 von Willebrand disease: Results from a multicenter European study (MCMDM-1 VWD). *J Thromb Haemost.* 2006;4(4):766-773.
10. Lenting PJ, Westein E, Terraube V, et al. An experimental model to study the in vivo survival of von Willebrand factor. basic aspects and application to the R1205H mutation. *J Biol Chem.* 2004; 279(13):12102-12109.

11. Mannucci PM, Lombardi R, Castaman G, et al. Von Willebrand disease "Vicenza" with larger-than-normal (supranormal) von Willebrand factor multimers. *Blood.* 1988;71(1):65-70.
12. Gezsi A, Budde U, Deak I, et al. Accelerated clearance alone explains ultralarge multimers in VWD Vicenza. *J Thromb Haemost.* 2010;8(6): 1273-1280.
13. Federici AB, Mazurier C, Berntorp E, et al. Biologic response to desmopressin in patients with severe type 1 and type 2 von Willebrand disease: Results of a multicenter European study. *Blood.* 2004;103(6):2032-2038.
14. Castaman G, Lethagen S, Federici AB, et al. Response to desmopressin is influenced by the genotype and phenotype in type 1 von Willebrand disease (VWD): Results from the European study MCMDM-1VWD. *Blood.* 2008;111(7):3531-3539.
15. O'Brien LA, James PD, Othman M, et al. Founder von Willebrand factor haplotype associated with type 1 von Willebrand disease. *Blood*. 2003; 102(2):549-557.
16. James PD, Notley C, Hegadorn C, et al. The mutational spectrum of type 1 von Willebrand disease: Results from a Canadian cohort study. *Blood.* 2007;109(1):145-154.
17. Bowen DJ, Collins PW. An amino acid polymorphism in von Willebrand factor correlates with increased susceptibility to proteolysis by ADAMTS13. *Blood.* 2004;103(3):941-947.
18. Keeney S, Grundy P, Collins PW, Bowen DJ. C1584 in von Willebrand factor is necessary for enhanced proteolysis by ADAMTS13 in vitro. *Haemophilia.* 2007;13(4):405-408.
19. Marx I, Christophe OD, Lenting PJ, et al. Altered thrombus formation in von Willebrand factor-deficient mice expressing von Willebrand factor variants with defective binding to collagen or GPIIbIIIa. *Blood.* 2008;112(3):603-609.
20. Rayes J, Hollestelle MJ, Legendre P, et al. Mutation & ADAMTS13-dependent modulation of disease severity in a mouse model for von Willebrand disease type 2B. *Blood.* 2010;115(23): 4870-4877.
21. Golder M, Pruss CM, Hegadorn C, et al. Mutation-specific hemostatic variability in mice expressing common type 2B von Willebrand disease substitutions. *Blood.* 2010;115(23):4862-4869.
22. Pruss CM, Notley CR, Hegadorn CA, O'Brien LA, Lillicrap D. ADAMTS13 cleavage efficiency is altered by mutagenic and, to a lesser extent, polymorphic sequence changes in the A1 and A2 domains of von Willebrand factor. *Br J Haematol.* 2008;143(4):552-558.
23. Shi CX, Graham FL, Hitt MM. A convenient plasmid system for construction of helper-dependent adenoviral vectors and its application for analysis of the breast-cancer-specific mammaglobin promoter. *J Gene Med.* 2006;8(4):442-51.
24. Vigna E, Amendola M, Benedicenti F, Simmons AD, Follenzi A, Naldini L. Efficient tet-dependent expression of human factor IX in vivo by a new self-regulating lentiviral vector. *Mol Ther.* 2005;11(5):763-775.
25. Kokame K, Matsumoto M, Fujimura Y, Miyata T. VWF73, a region from D1596 to R1668 of von Willebrand factor, provides a minimal substrate for ADAMTS-13. *Blood.* 2004;103(2):607-612.
26. Plaimauer B, Zimmermann K, Volkel D, et al. Cloning, expression, and functional characterization of the von Willebrand factor-cleaving protease (ADAMTS13). *Blood.* 2002;100(10):3626-3632.
27. Kato S, Matsumoto M, Matsuyama T, Isonishi A, Hiura H, Fujimura Y. Novel monoclonal antibody-based enzyme immunoassay for determining plasma levels of ADAMTS13 activity. *Transfusion.* 2006;46(8):1444-1452.
28. Stakiw J, Bowman M, Hegadorn C, et al. The effect of exercise on von Willebrand factor and ADAMTS-13 in individuals with type 1 and type 2B von Willebrand disease. *J Thromb Haemost.* 2008;6(1):90-96.
29. Bruno K, Volkel D, Plaimauer B, et al. Cloning, expression and functional characterization of the full-length murine ADAMTS13. *J Thromb Haemost.* 2005;3(5):1064-1073.
30. Denis C, Methia N, Frenette PS, et al. A mouse model of severe von Willebrand disease: Defects in hemostasis and thrombosis. *Proc Natl Acad Sci U S A.* 1998;95(16):9524-9529.
31. Dubois C, Panicot-Dubois L, Merrill-Skoloff G, Furie B, Furie BC. Glycoprotein VI-dependent and -independent pathways of thrombus formation in vivo. *Blood.* 2006;107(10):3902-3906.
32. Gavins FN, Chatterjee BE. Intravital microscopy for the study of mouse microcirculation in anti-inflammatory drug research: Focus on the mesentery and cremaster preparations. *J Pharmacol Toxicol Methods.* 2004;49(1):1-14.
33. Chitta MS, Duhe RJ, Kermode JC. Cloning of the cDNA for murine von Willebrand factor and identification of orthologous genes reveals the extent of conservation among diverse species. *Platelets.* 2007;18(3):182-198.
34. Varadi K, Rottensteiner H, Vejda S, et al. Species-dependent variability of ADAMTS13-mediated proteolysis of human recombinant von Willebrand factor. *J Thromb Haemost.* 2009;7(7):1134-1142.
35. Banno F, Kaminaka K, Soejima K, Kokame K, Miyata T. Identification of strain-specific variants of mouse Adamts13 gene encoding von Willebrand factor-cleaving protease. *J Biol Chem.* 2004;279(29):30896-30903.
36. Banno F, Chauhan AK, Kokame K, et al. The distal carboxyl-terminal domains of ADAMTS13 are required for regulation of in vivo thrombus formation. *Blood.* 2009;113(21):5323-5329.